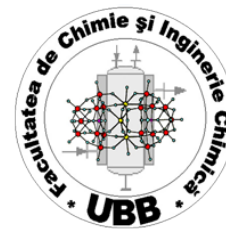**Faculty of Chemistry and Chemical Engineering**
Babeș-Bolyai University, Cluj-Napoca

_____

SZŐKE ÁRPÁD FERENC

Polymer-modified surfaces for electroanalytical applications and anticorrosive protection

PhD Thesis
Abstract

Scientific advisor
Prof. Dr. Liana Maria Mureşan

2019

Table of contents

Keywords: electrochemical sensors, electrocatalysis, ascorbic acid, hydrogen peroxide, nafion, anticorrosive protection, chitosan, dip-coating

Introduction

The practical application of polymers is a challenging task. They present several advantages such as cost efficiency and adaptability to different environments through physical and chemical modifications, resulting in a wide range of applications. The disadvantage of such systems can be their reproducibility (due to a large number of variables influencing the manufacturing process) and their stability under stress.

The well-known applications of polymers include the production of different objects (ranging from the toy industry to biomedical appliances), coating-production, water purification, molecular recognition, etc. Polymers are also important in the field of electrochemistry, where they are extensively used in conductive and insulating coatings, inhibitors, immobilization and selective electroanalysis.

In this context, this thesis focuses on two distinct research directions, both regarding the use of polymers, in particular, chitosan and Nafion. These are (**i**) the preparation of electrochemical sensors for hydrogen peroxide and ascorbic acid; and (**ii**) the preparation of corrosion-resistant coatings for the protection of zinc substrates.

(i) Electrochemical sensors

In the first research direction of this thesis, chitosan and Nafion polymers are used as immobilization matrices for redox mediators and modifying agents. This work focuses on the electroanalytical detection of hydrogen peroxide and ascorbic acid at glassy carbon electrode interfaces modified with (i) reduced graphene oxide/myoglobin immobilized with chitosan, and (ii) graphene oxide/gold nanoparticles immobilized with Nafion.

Compared to classical analytical methods, electrochemical investigations have several advantages, including the simplicity and speed of detection, as well as the possibility of real-time monitoring. As electrochemical methods are highly applicable in the detection of analytes with biological relevance, modified electrode-development maintains great importance in the field of electrochemistry.

Glassy carbon electrodes are often used in electroanalysis, however, pronounced fouling effects can manifest in the case of analytes with redox peaks at high or low potentials, due to the electrode material becoming unstable under the conditions of reduction or oxidation. This

phenomenon can be countered by the application of electrocatalytic agents such as graphenes or noble metal nanoparticles, which can reduce the oxidation potential and increase the reduction potential of the studied analyte, by mediating the electron transfer. The increased active surface area of such modified electrodes also results in improved sensitivity of detection.

(ii) Anticorrosive coatings

In the second and third research directions of this thesis, chitosan is used as a protective barrier against corrosion. This study includes the production and characterization (including an applicability assessment) of modified chitosan-based anticorrosive coatings produced with dip-coating and electrophoretic deposition for the improved protection of zinc substrates.

Corrosion is a global problem and an important source of economic loss. It is a natural phenomenon, defined as the (usually oxidative) degradation process of metals, polymers, ceramics or other materials. Corrosion can negatively impact the mechanical, electrochemical and visual aspect of metal objects, endangering the structural integrity of building and vehicles; deteriorating the functionality of electrical appliances and cables; ruining the visual aspect of decorations and jewelry. A number of different techniques are used to improve the corrosion resistance of metals, including coating, cathodic protection, anodic protection and the use of different corrosion inhibitors.

The application of polymeric coatings is a well-established discipline. Nevertheless, due to the abundance of plastic waste produced by the population, and their versatility, the use of biopolymers in anticorrosive protection is gaining significant momentum. Such coatings have great potential in the temporary protection of metals due to their biodegradability. Additionally, being simple to modify with different additives and co-polymers, they are highly adaptable to different systems, including biomedical use.

This thesis is structured in two parts: (**i**) a theoretical part, which includes a **Bibliographic overview**, containing literature data and a description of the methods used for sample preparation and characterization; (**ii**) the **Original contribution** of the research, which includes methodology, results, and conclusions for each of the three research directions described above. The thesis also enumerates scientific contributions during the PhD studies in the form of conference presentations and scientific articles.

Bibliographic overview

1. Electrochemical sensors

Electrochemical sensors convert the information obtained from electrochemical reactions into an analytically useful signal that is applicable in the qualitative and quantitative characterization of a system [Shetti et al., 2019; Antuña-Jiménez et al., 2012].

Although they have several advantages compared to other methods, the overlap of redox peaks in the case of analytes with similar redox potentials [Szoke et al., 2019c] and the instability of the electrode material itself can lead to errors in detection. Consequently, the electron transfer between the electrode material and the studied analyte is often mediated with additives that show electrocatalytic activity [Shao et al., 2016].

1.1. Mediated electron transfer

Redox mediation is a relatively simple concept. In this process, surface-immobilized sites are activated by a voltage applied to the support electrode. These sites then oxidize or reduce other redox agents located in the solution phase adjacent to the immobilized layer can greatly improve results when the direct oxidation or reduction at the electrode surface is inhibited [Lyons, 2015].

1.2. Graphenes

Graphene is a nanomaterial, consisting of two-dimensional layers of carbon atoms with sp^2 hybridization, connected in a hexagonal lattice structure [Siqueira and Oliveria, 2017]. Graphenes also show good electrocatalytic activity and synergistic effects when used in conjunction with noble metal nanoparticles [Szoke et al., 2019c].

1.3. Hydrogen peroxide sensor

1.3.1. Hydrogen peroxide

Hydrogen peroxide has importance in living organisms, as it has a role in cellular signaling pathways and is produced as a destructive oxidant to ward off pathogens [Lin, 2013]. Due to weak electron transfer kinetics, the determination of H_2O_2 on bare glassy carbon electrodes cannot be achieved with high sensitivity; consequently, electrocatalytic agents and proteins with peroxidase activity were tested to improve results [Szoke et al., 2016].

1.3.2. Myoglobin

Myoglobin serves as an oxygen reservoir, providing oxygen when, during periods of intense muscular activity, blood oxygen delivery is insufficient [Harvey, 2008]. Myoglobin has peroxidase activity and is widely used in investigating electron transfers, however, due to the deeply buried redox center in the Mb macromolecule, the direct electron transfer between the protein and the bare electrode is inefficient [Szoke et al., 2016].

1.4. Ascorbic acid sensor

1.4.1. Ascorbic acid

L-ascorbic acid (vitamin C) is a vitamin and antioxidant found in plants, that also serves important functions in the human body. Due to the compound's significance, the quantitative detection of AA in biological and non-biological samples is of great importance. The relatively high oxidation potential, and the overlapping oxidation peaks of coexisting species render analysis by electrochemical methods problematic [Szoke et al., 2019c]. Results can be improved by using graphenes alone or in conjunction with other materials.

1.4.2. Gold nanoparticles

Gold nanoparticles are often used electrocatalysts, due to controllable particle size and synergistic effects with other electrocatalytic agents, such as graphenes. Due to their versatility, they are used for several applications: electron transfer mediators [Szoke et al., 2019c], drug delivery [Chandran and Thomas, 2015], nanoplasmonics [Asahi et al.; 2006] and catalysis [Kerdi et al., 2010]. The synergistic effect observed between gold nanoparticles and different type of graphenes renders them an attractive candidate in electrocatalysis.

2. Anticorrosive protection

The global economic loss due to corrosion is estimated at 3.4% of the GDP, or 2.2 trillion € annually. The phenomenon has a great impact on the services, production and agricultural industries of all countries, however, this effect can be reduced by the implementation of proper protection methods [Koch et al., 2016]. Polymeric coatings offer a good alternative in eco-friendly corrosion protection, however, modification through the incorporation of materials

[Ching et al.; 2019] or copolymerization [Feng and Iroh, 2017] is necessary to obtain films with good protective capabilities. In this regard, one of the most studied polymers is chitosan.

2.1. Chitosan coatings

Chitosan is the β-(1,4)-linked polysaccharide of D-glucosamine. It is a water-soluble polymer produced by the partial deacetylation of chitin (originating from natural sources). Chitosan is considered a versatile polymer [Szőke et al., 2019a; Szőke et al., 2019b], used for many different applications. The modest barrier properties of chitosan coatings can be improved by forming polymer composites [Pang and Zhitomirsky, 2008] or through crosslinking [Szőke et al., 2019b]. Alternatively, the positive charge of chitosan can be used to accumulate negatively charged inhibitors that can adsorb directly on the metal surface, resulting in improved protection with reduced need for raw materials.

2.2. Modified chitosan coatings

In order to improve the modest barrier properties of the native chitosan coatings, different additives were impregnated into the polymer matrix.

2.2.3. Indigo carmine

Indigo carmine is a water soluble 5,5′-indigodisulfonic acid sodium salt. It is non-toxic and widely used as a food colorant under the name E132 [Food Standards Agency, 2019], as well as in medicine as an indicator of renal function [Deture and Brylie, 1974]. As a result of the two negative charges on either side of the molecule, indigo carmine shows high affinity towards chitosan [dos Anjos et al., 2002].

2.2.4. Ammonium paratungstate

Ammonium paratungstate (PTA) is a non-toxic and water-soluble crystalline complex salt. Similarly to IC, it can be impregnated into chitosan films. The size of the molecule decreases any possible leaching of the PTA from the modified chitosan coatings, however, the impregnation process can also be hindered due to the same characteristics.

2.2.5. 2-acetylamino-5-mercapto-1,3,4-thiadiazole

2-acetylamino-5-mercapto-1,3,4-thiadiazole (AcAMT), is a non-toxic organic molecule, considered an acetazolamide intermediate with limited applicability. Positive results were obtained with AcAMT in the anticorrosive protection of bronze [Chelaru and Muresan, 2014]. In neutral or slightly acidic conditions, a notable amount of AcAMT is negatively charged [Instant Cheminformatics Solutions, 2019]. Consequently, it can be possible to accumulate AcAMT in chitosan layers, increasing the inhibitor concentration in the proximity of the metal surface.

3. Preparation methods of polymeric coatings

Polymer coatings are thin films applied to either flat substrates or irregular objects. Their use in the immobilization of different materials is of particular importance, due to the numerous applications of such composites in catalysis [Shi et al., 2012; Mirkhalaf and Graves, 2012; Song et al., 2014], optics [Griffete et al., 2012; Mohr, 2006], biomedicine [Thissen, 2016; Bovin and Gabius, 1994], etc. Nanoparticles used as electrocatalytic agents are often immobilized with Nafion or chitosan.

Native and modified polymer coating can also be applied to a metal surface to provide anticorrosive protection. Such coatings are often modified by crosslinking agents, copolymerization or other additives to improve applicability.

3.1. Drop casting technique

The most commonly used technique to prepare modified electrodes is drop casting [Eng et al., 2015; Hanifah et al., 2018], favored due to its versatility, tunability and simplicity. It consists of obtaining thin layers by dropping a solution or dispersion onto a surface and evaporating the solvent. The technique is used with great success in the case of glassy carbon electrodes.

3.2. Dip-coating technique

Dip-coating is a process in which the substrate is immersed in a liquid and then lifted out at a preset speed controlled by a continuous motor [Schwarz and Langenhove, 2013]. It is highly efficient in producing thin polymer coatings with well-controlled characteristics for anticorrosive protection and controlled release of impregnated species [Dabóczi et al., 2016; Albert et al., 2015].

3.3. Electrophoretic deposition

Electrophoretic deposition is a term used for a broad range of industrial processes which include electrocoating, cathodic electrodeposition, anodic electrodeposition, e-coating and electrophoretic coating, or electrophoretic painting [Quintino, 2014]. It is a two-step process in which the particles suspended in a colloid solution are collected onto a substrate with the application of an electric field.

4. Non-Electrochemical methods of analysis

4.1.1. Optical microscopy

Optical microscopes use visible light and a system of lenses to magnify images of small samples. The image from an optical microscope can be captured by cameras.

4.1.2. Transmission electron microscopy

Transmission electron microscopy (TEM) is widely used in the characterization of different nanoparticles and membranes. Due to its functionality being based on electron beams, rather than light beams, very high resolutions can be obtained.

4.1.3. Scanning electron microscopy

Scanning electron microscopy is used to study the particle size, shape, and texture of materials. In SEM, a beam of electrons scans across the sample in a series of parallel tracks. The electrons interact with the sample and produce different signals which can be detected and displayed on the screen of a cathode ray tube. Since the depth of focus is much greater than that of the light microscope, information on surface morphology can be generated [Amidon et al., 2017].

4.1.4. Atomic force microscopy

Atomic force microscopy is based on scanning a sharp tip (with a typical end diameter of 5–10 nm) over then analyzed surface, producing topographical images, used to study surface morphology on a very small scale [Bastidas et al., 2011].

4.2.1. UV-Vis spectroscopy

UV-Vis spectroscopy consists of measuring the transmittance (absorbance) or reflectance of samples. It can be used on solutions, gases or in rare cases, solid samples. During irradiation of a sample, part of the light is absorbed, part of it is transmitted through the sample, while some may be reflected [Kekedy and Kekedy, 1995].

4.2.2. Infrared and Raman spectroscopy

Infrared spectroscopy depends upon vibrations involving changes in permanent dipole moments during excitation. These vibrations can be symmetric or antisymmetric stretching, rocking, wagging, scissoring and twisting. Usually, the so-called mid-IR region is studied, which ranges between *ca.* 4000–400 cm^{-1}.

Raman spectroscopy monitors shifts in the frequency of scattered light due to alterations in bond polarizability, resulting from interactions with different vibrational modes [Bhambhani et al., 2012]. It has some advantages, as it can be used for aqueous solutions and requires less sample preparation than infrared spectroscopy [Le Pevelen, 2017].

4.2.3. Energy-dispersive X-ray spectroscopy

Energy-dispersive X-ray spectroscopy (EDX,) is a surface analytical technique. An electron beam (typically in the range of 10-20 keV) hits the sample, exciting an electron in an inner electron shell, emitting characteristic X-ray signals of the studied sample's atomic structure. By assigning the appropriate elements to the obtained spectrum, the elemental composition and mapping of the sample surface can be analyzed [Ebnesajjad, 2014; Polini and Yang, 2017].

4.3. Wettability analysis. Sessile drop and captive bubble methods

Determining wetting properties can give valuable information on the interaction between a polymer coating and the surrounding environment. The quantitative monitoring of the wetting process can be done *via* the contact angle. This is the angle the droplet makes with the substrate, measured through the liquid in question [Lotfi et al., 2013]. Usually, the goniometry method is used, where the drop shape is captured by a camera.

4.4. Total organic carbon content analysis

Total organic carbon content analysis measures the total amount of carbon in a sample and subtracts the amount of inorganic carbon, resulting in the amount of organic carbon in a given sample.

4.5. Zeta potential and particle size analysis

Zeta potential is a measure of surface charge. It has great importance in the stability of a colloidal system. Large zeta potentials (larger than ± 30 mV) result in stronger repulsive forces between nanoparticles, resulting in a more stable colloid [Krstic et al., 2018].

The stability of a colloid solution and changes occurring over time can be monitored through particle size analysis, by dynamic light scattering [Berne and Pecora, 2000]. The method is based on fluctuations in the light scattering intensity of a colloidal solution due to Brownian motion.

5. Electrochemical methods

5.1. Cyclic voltammetry

Cyclic voltammetry is used to study simple redox processes in organic and inorganic chemistry, as well as to the characterize multielectron-transfer processes in biochemistry and macromolecular chemistry [Heinze, 1984]. Its uses cover characterization, synthesis, mechanisms, and analysis [Chooto, 2018]. CV experiments offer thermodynamic parameters (redox potential), as well as direct insights into the kinetics of electrode reactions [Heinze, 1984]. CV measurements consist of a time-dependent linear potential cycling while recording the resulting signal: the current (or current density).

5.2. Amperometry

Amperometry is the monitoring of the gain (reduction) or loss (oxidation) of electrons in the presence of a fixed potential by measuring changes in current [Hanson et al., 2005] at the working electrode. Amperometry is a method better suited for the quantitative detection of analytes than cyclic voltammetry, with low limits of detection and tunable selectivity, by choosing an applied potential that is discriminate against other analytes [Hanson et al., 2005].

5.3. Electrochemical impedance spectroscopy

Impedance spectroscopy measures the electrical resistance and capacitance of a material *via* application of a sinusoidal AC excitation signal. An impedance spectrum is obtained by varying the frequency of the AC signal over a defined range. The capacitance and resistance of the system can be calculated by measuring the in-phase and out-of-phase current responses [Honeychurch, 2012]. Impedance spectroscopy is widely used in electroanalytical, biology and corrosion studies. Nyquist impedance curves (plotting the imaginary part of the impedance in the function of the real part) is used to explain the mechanism of electron transfer by attributing an equivalent circuit to the curve.

5.4. Polarization studies

The interpretation of polarization curves is used to study the mechanism, corrosion rate and susceptibility of materials to corrosion in a well-defined environment. Linear polarization studies are used to determine the polarization resistance (Rp).

Plotting the potential in the function of lgi results in a semilogarithmic polarization curve. By fitting lines to the anodic and cathodic region of these polarization curves, the Evans diagram can be obtained [Palm Sens, 2019] and consequently the Tafel coefficients.

Original contribution

Objectives of the thesis
The main research directions of this thesis are the following:

1. **Modified glassy carbon electrodes produced with the drop casting method**
   - Improvement of the electron transfer properties of glassy carbon interfaces by modification through the immobilization of reduced graphene oxide, noble metal nanoparticles and proteins on the electrode surface with Nafion or chitosan polymers
   - Optimization and electroanalytical characterization of the obtained modified glassy carbon electrodes for the detection of analytes with biological importance (H_2O_2 and ascorbic acid)

2. **Anticorrosive chitosan-based coatings produced by dip-coating on zinc substrates**
   - Application of chitosan coatings by the dip-coating method on zinc substrates

- Impregnation of the chitosan coatings to improve anticorrosive properties by reducing the permeability of the polymer films through (**i**) ionic crosslinking [dos Anjos et al., 2002; Berger et al., 2004] (with indigo carmine or ammonium paratungstate); or (**ii**) adsorption (with 2-acetylamino-5-mercapto-1,3,4-thiadiazole, by using the chitosan to channel high amounts of corrosion inhibitor towards the metal surface, in order to obtain anticorrosive effects [Chelaru and Muresan, 2014; Varvara et al., 2008])(Figure 28)
- Characterization and applicability assessment of the impregnated chitosan coatings by different methods
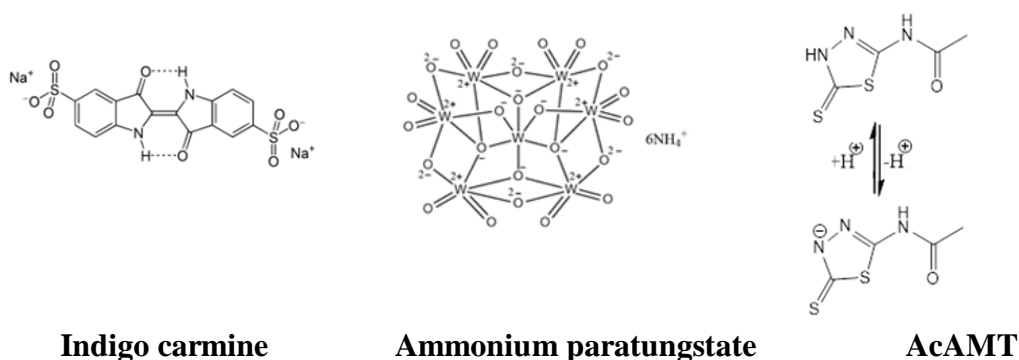

Indigo carmine   **Ammonium paratungstate**   **AcAMT**

Figure 28: Different impregnating agents used to improve the anticorrosive properties of chitosan coatings

3. **Anticorrosive silica-chitosan nanoparticle coatings produced by electrophoretic deposition on zinc substrates**
    - Production of chitosan covered silica-nanoparticle dispersions
    - Using the prepared dispersions to coat zinc substrates by electrophoretic deposition
    - Characterization and applicability assessment as a possible anticorrosive barrier of the nanoparticle-chitosan coatings by electrochemical and microscopy techniques

1.2. Glassy carbon electrode modified with rGO, myoglobin and chitosan (GCE/Chit/Chit-rGO-Mb) as a H_2O_2 sensor

A GCE/Chit/Chit-rGO-Mb electrode was produced by the drop casting method as a possible modified interface for the detection of H_2O_2.
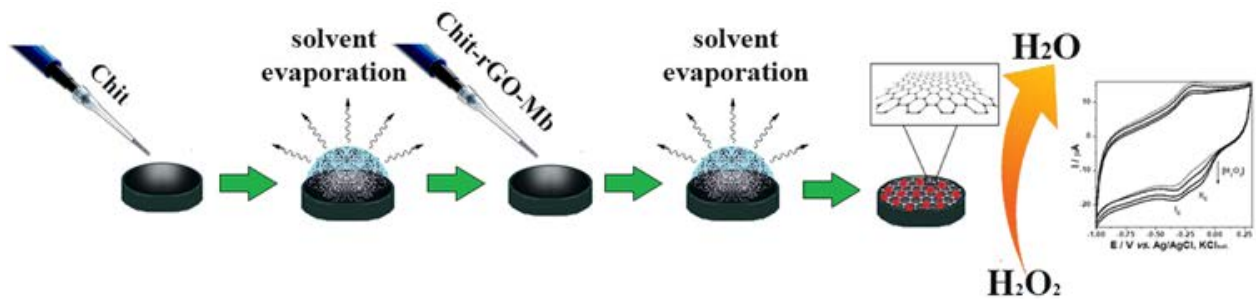
1.2.2. Optimization study

The optimization study was directed towards the optimization of the amount if (**i**) rGO and (**ii**) Mb.

The highest peak current was obtained for the maximum deposited amount of 5 µg rGO (Figure 33 A). The sensitivity of hydrogen peroxide detection showed a maximum at 40 µg Mb, which was thus used for further studies [Szoke et al., 2017].
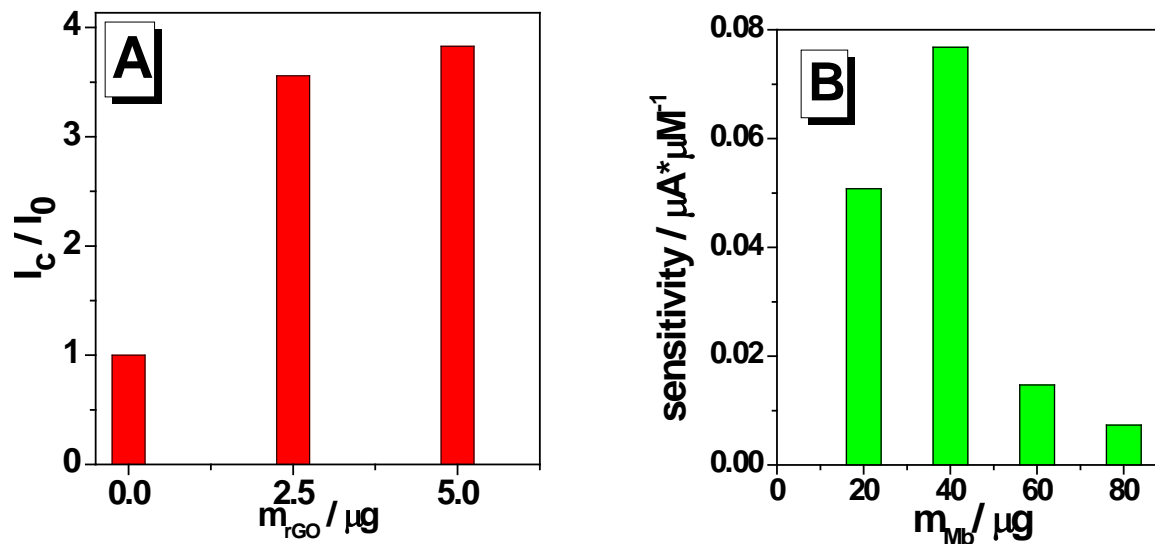

Figure 33: Influence of the: amount of rGO deposited on the electrode surface on the

*peakreduction currents for the detection of 10 µM H₂O₂ (**A**);*
amount of Mb deposited on the electrode surface on the
*sensitivity of H₂O₂ detection (**B**)*

Experimental conditions: PBS (pH=7), scan rate, 50 mV/s

1.2.3. Electrode characteristics and analytical performance

The *permeability* of the modifying layer was studied using electrochemical impedance spectroscopy [Raicopol et al., 2012]. The electrical equivalent circuits best fitting the impedance spectra were $R(Q_1R_1)$ for the modified electrodes and $R(Q_1R_1)W$ for the bare GCE.

The presence of the chitosan layer determines an increase of the charge transfer resistance for the samples containing the polymer: 3234 Ωcm^2 for GCE/Chit/Chit-Mb and 3009 Ωcm^2 for GCE/Chit/Chit-rGO-Mb, compared to 1848 Ωcm^2 for the bare GCE electrode. This points to chitosan acting as a permeable barrier to $K_3[Fe(CN)_6]$.

The logarithm of the peak currents (log I) shows a linear dependency to the logarithm of the scan rate (log v) for both oxidation and reduction processes. The slopes were also similar (around 0.7), indicating mixed kinetics (diffusion-adsorption) at the electrode-solution interface [Szoke et al., 2017].

The *electrocatalytic effect* of the modified GCE/Chit/Chit-rGO-Mb electrode was studied by cyclic voltammetry (Figure 36). After the addition of H_2O_2, an additional reduction peak (II$_C$) at -150 mV *vs.* Ag/AgCl, KCl$_{sat}$ was observed. This was attributed to the reduction of hydrogen peroxide at the active site of the heme group of the Mb immobilized on the electrode surface.

Plotting the second reduction peak, a good linear in the range of 10 - 30 µM was observed. The sensitivity of the GCE/Chit/Chit-rGO-Mb modified electrode was found to be significantly higher (0.0815 µA/µM, R^2=0.9881) than that of the GCE/Chit/Chit-Mb modified electrode (0.0394 µA/µM, R^2=0.9859). Immobilizing rGO at the electrode surface also slightly reduced the detection limit of H_2O_2 from 7.75 µM to 7.09 µM [Szoke et al., 2017]
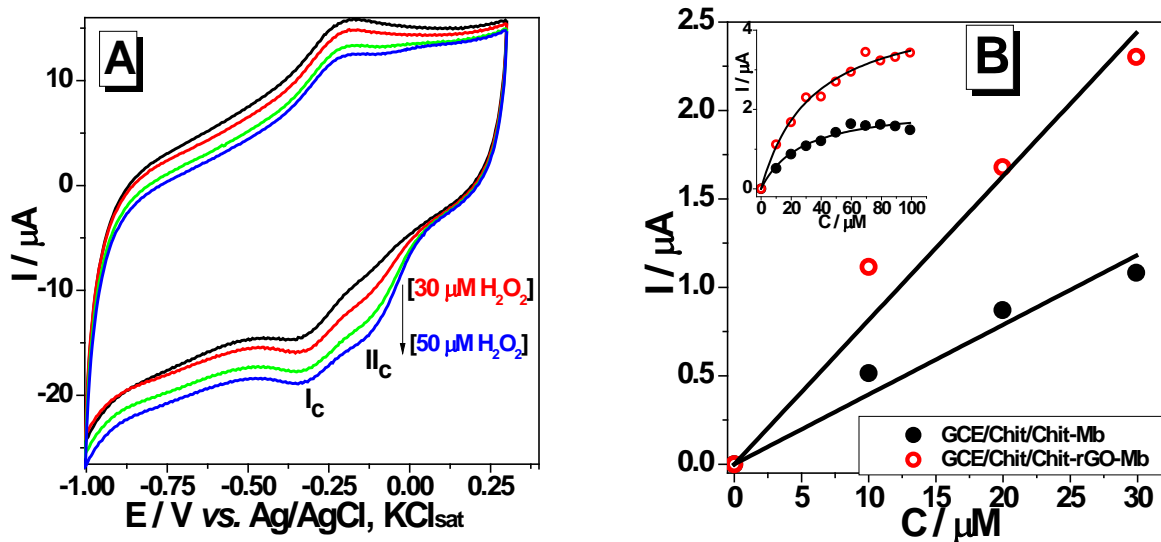
*Figure 36: **A**: Cyclic voltammograms measured at a GCE/Chit/Chit-rGO-Mb modified electrode, recorded in the absence of H_2O_2 (**black line**) and in the presence of different amounts (up to 50 µM) of H_2O_2 (**colored lines**).*

*   **B**: Calibration curves obtained for the reduction of H_2O_2 at GCE/Chit/Chit-Mb (black ●) and GCE/Chit/Chit-rGO-Mb (red ◯) modified electrodes.*

Experimental conditions: PBS (pH=7); starting potential +0.3 V vs. Ag/AgCl, KCl$_{sat}$; scan rate, 50 mV/s.

1.3. Partial conclusions - H_2O_2 sensor

The addition of reduced graphene oxide increases the active surface area, improving the activity of Mb. The overlapping of the reduction peaks of Mb and H_2O_2 can be an issue, however, the modified GCE/Chit/Chit-rGO-Mb was successfully applied for H_2O_2 detection. The presence of rGO improved results.

1.4. Glassy carbon electrode modified with gold nanoparticles, erGO and Nafion (GCE/AuNPs-erGO-Nafion) as an ascorbic acid sensor

A modified electrode interface was prepared by drop casting gold nanoparticles and graphene oxide (immobilized with Nafion) on a glassy carbon electrode surface. The electrode was activated by potential cycling to reduce the GO into erGO.
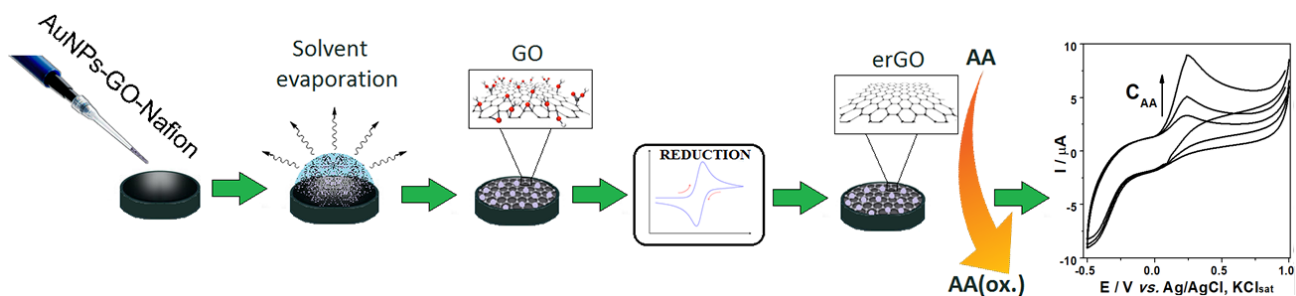
1.4.2.1. *Drop casting mixture composition*

The optimization study was conducted to determine the optimal amount of (**i**) GO, (**ii**) AuNPs and (**iii**) Nafion, in order to obtain an ideal composition of the modified electron transfer interface. The ideal amounts of each modifying agent were: 5 μL AuNPs sol, 2.5 μL GO dispersion and 5 μg Nafion as an immobilizing agent.

1.4.4.1. *Electrocatalytic effect of GCE/AuNPs-erGO-Nafion interface*

Compared to the position of the oxidation peak of ascorbic acid at the bare GCE electrode (*ca.* +650 mV *vs.* Ag/AgCl, KCl$_{sat}$), the oxidation potential of AA at the modified GCE/AuNPs-erGO-Nafion electrode was observed at +250 mV *vs.* Ag/AgCl, KCl$_{sat}$. This shift of around 400 mV, together with an increase of the oxidation current, suggests a strong electrocatalytic activity of the modified AuNPs-erGO-Nafion interface (Figure 42 B).
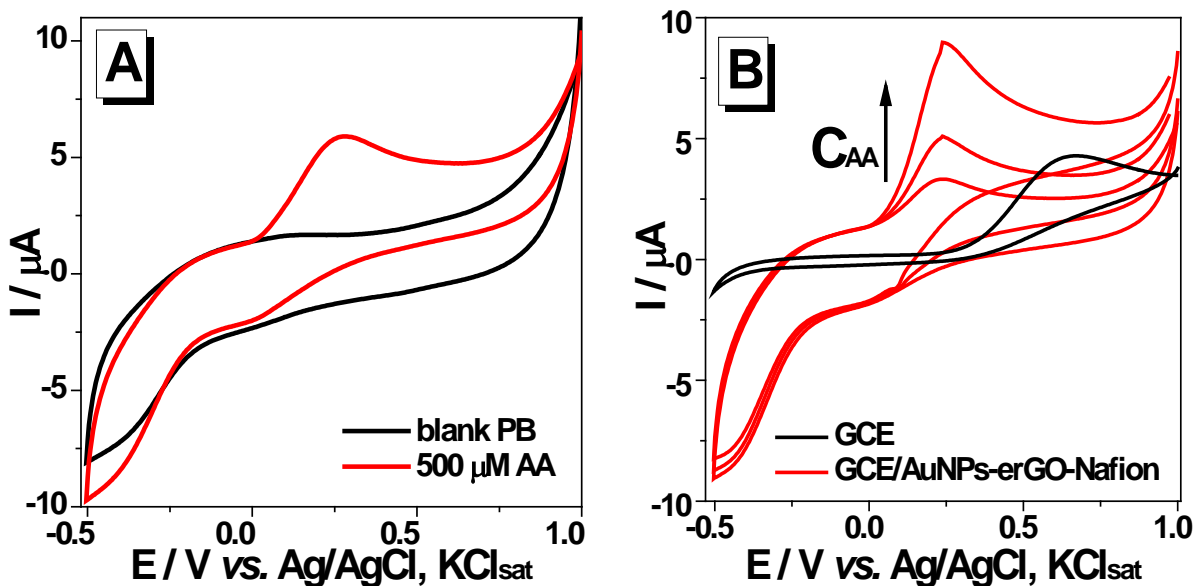
Figure 42: Cyclic voltammetry response of:

*A: GCE/AuNPs-erGO-Nafion modified electrode in the absence (**black line**) and in the presence of 500 μM AA (**red line**)*

*B: bare GCE (**black line**) in the presence of 500 μM AA and GCE/AuNPs-erGO-Nafion (**red lines**) in the presence of 250, 500 and 1000 μM AA.*

Experimental conditions: electrolyte, 0.1 M PBS (pH=7); starting potential, +1.0 V vs. Ag/AgCl, KClsat; scan rate, 50 mV/s.

1.4.4.6.   *Amperometry*

The analytical performance of the GCE/AuNPs-erGO-Nafion modified electrode was studied by batch amperometry (Figure 47). The calibration curve shows a good linear relationship between the steady-state current and the concentration of AA at a linear domain of 5 – 30 µM with a sensitivity of 39.07 ± 1.36 µA/mM. The determined LOD (with a signal to noise ratio of 3) for AA showed a good value of 2.76 µM AA.

Figure 47: Amperometric calibration curve of AA, determined at a GCE/AuNPs-erGO-Nafion modified electrode

Experimental conditions: electrolyte, 0.1 M PBS (pH=7); applied potential, +0.1 V vs. Ag/AgCl, KCl$_{sat}$; rotating speed, 500 rpm.
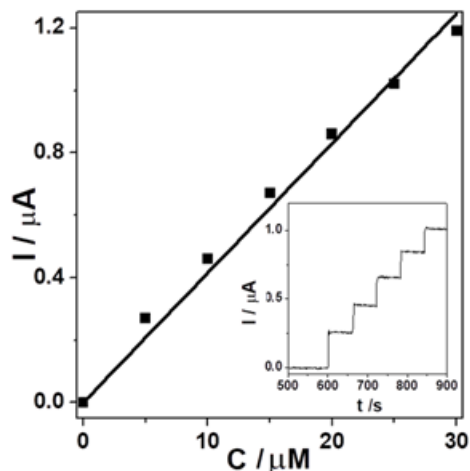
1.4.4.7.   *Real samples analysis*

To test the applicability of the GCE/AuNPs-erGO-Nafion modified electrode for biomedical use, batch amperometry was used to determine the AA concentration in real samples, namely three different ascorbic acid-containing pharmaceutical products, chosen as a representative group of the trends in modern medicine and food supplements.

The obtained concentrations were compared to the nominal concentrations of each product to determine recovery (Figure 48 and Table 3). The good recovery value obtained for the Béres vitamin C tablet (103.22 ± 0.78%) was possible due to a low amount of electroactive additives present in the studied pharmaceutical product. In the case of the Laropharm and Redoxon tablets, higher recovery values were obtained (118.23 ± 1.13% and 141.40 ± 0.75%, respectively). This is probably due to the high amounts of propolis (Laropharm tablet) and beta-carotene (Redoxon effervescent tablet) additives present in the samples, which show wide-range oxidation peaks at potentials around 400 mV [Belfar et al., 2015; Ziyatdinova et al., 2012] and could interfere with AA detection.
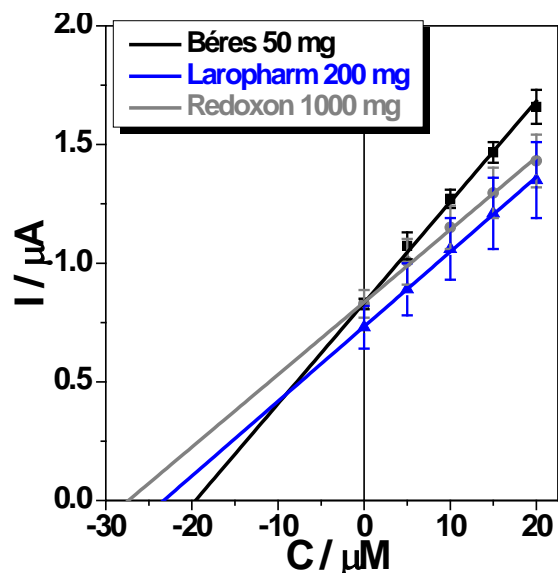
*Figure 48. Amperometric determination of the AA content at GCE/AuNPs-erGO-Nafion modified electrodes of pharmaceutical products using the standard addition method: Béres vitamin C tablet (**black** ■), Laropharm propolis tablet (**blue** ▲), Redoxon effervescent tablet (**grey** ●).*

Experimental conditions: electrolyte, 0.1 M PBS (pH=7); applied potential, +0.1 V vs. Ag/AgCl, KCl$_{sat}$; rotating speed, 500 rpm.

Table 3: Determination and recovery of AA in pharmaceutical products.

Samples containing ascorbic acid from:	Concentration added (µM)	Concentration found (µM)	Recovery (%)	R^2 / N
Béres	**20**	**20.65 ± 0.16**	**103.22 ± 0.78**	**0.9982 / 5**
Bayer-Redoxon	20	28.28 ± 0.15	141.40 ± 0.75	0.9976 / 5
Laropharm	20	23.65 ± 0.23	118.23 ± 1.13	0.9989 / 5

1.5.   Partial conclusions – ascorbic acid sensor

Cyclic voltammetry was used to determine the optimal ratio of modifying agents (5 µL AuNPs, 2.5 µL GO and 5 µg of Nafion) and to study the electrocatalytic effect of the modified electron transfer interface on AA oxidation. A potential shift of *ca.* 400 mV and a slight increase in the peak currents shows that the composite matrix has a strong electrocatalytic effect, which

was attributed to the electron transfer mediating effect of AuNPs and the increased surface area provided by erGO. Results showed a linear domain between 5 - 30 µM of the AA calibration curve, with a detection limit of 2.76 µM AA. The new modified electrode was used successfully for AA detection in real samples.

2.   Chitosan-based anticorrosive coatings

The second research direction presented in the thesis is the preparation and characterization of chitosan coatings with improved anticorrosive protection abilities, prepared by the dip-coating method on zinc substrates (Figure 51).

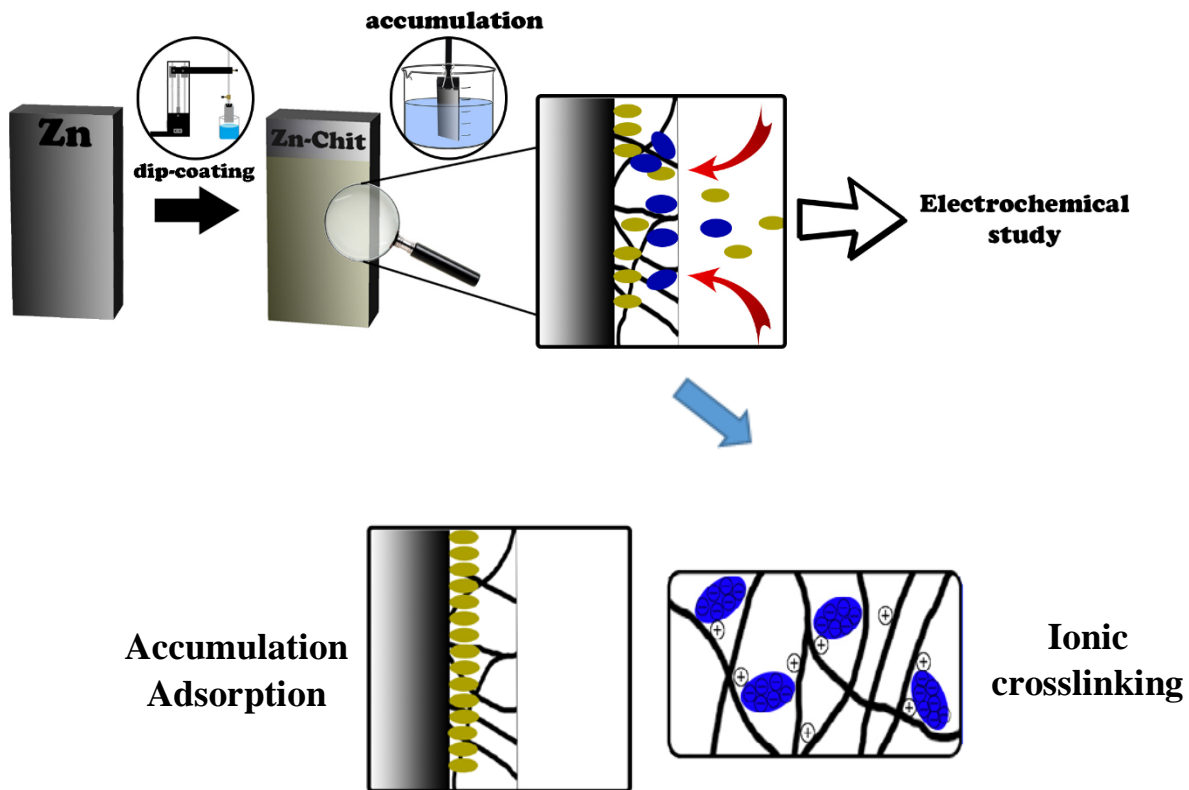*Figure 51: Preparation of Zn/Chit, Zn/Chit-IC, Zn/Chit-PTA and Zn/Chit-AcAMT systems by dip-coating and inhibitor accumulation.*

The expected inhibition effect can be obtained through two different routes: either ionic crosslinking (with polyanions) of the chitosan matrix or the adsorption of the accumulated corrosion inhibitor on the zinc surface (with inhibitors that show affinity to the metal surface).

2.2.2.1. *Layer thickness*

The layer thickness and refractive index of the Chit layers were determined by fitting a thin layer optical model [Hild et al., 2007; Szőke et al., 2019a; Szőke et al., 2019b] to the experimental transmittance data after adjustments.

2.2.3.2. *Stability of the impregnated systems*

The stability of the Chit-IC, Chit-PTA and Chit-AcAMT systems was tested on glass and quartz substrates by immersing multiple samples in distilled water. The stability of the systems was studied by following the amount of retained inhibitor (at a point in time) compared to the initial amount. From Figure 57, it can be concluded that both IC and PTA form stable systems with chitosan, most probably due to an ionic crosslinking effect. The minimal deviations of less than 4% can be attributed to small differences in the thickness of the chitosan coating [Szőke et al., 2019a; Szőke et al., 2019b]. A steep drop was noted in inhibitor amount for Chit-AcAMT coatings. This suggests a fast leaching of the modifying agent due to weaker ionic interactions compared to the Chit-IC and Chit-PTA systems.
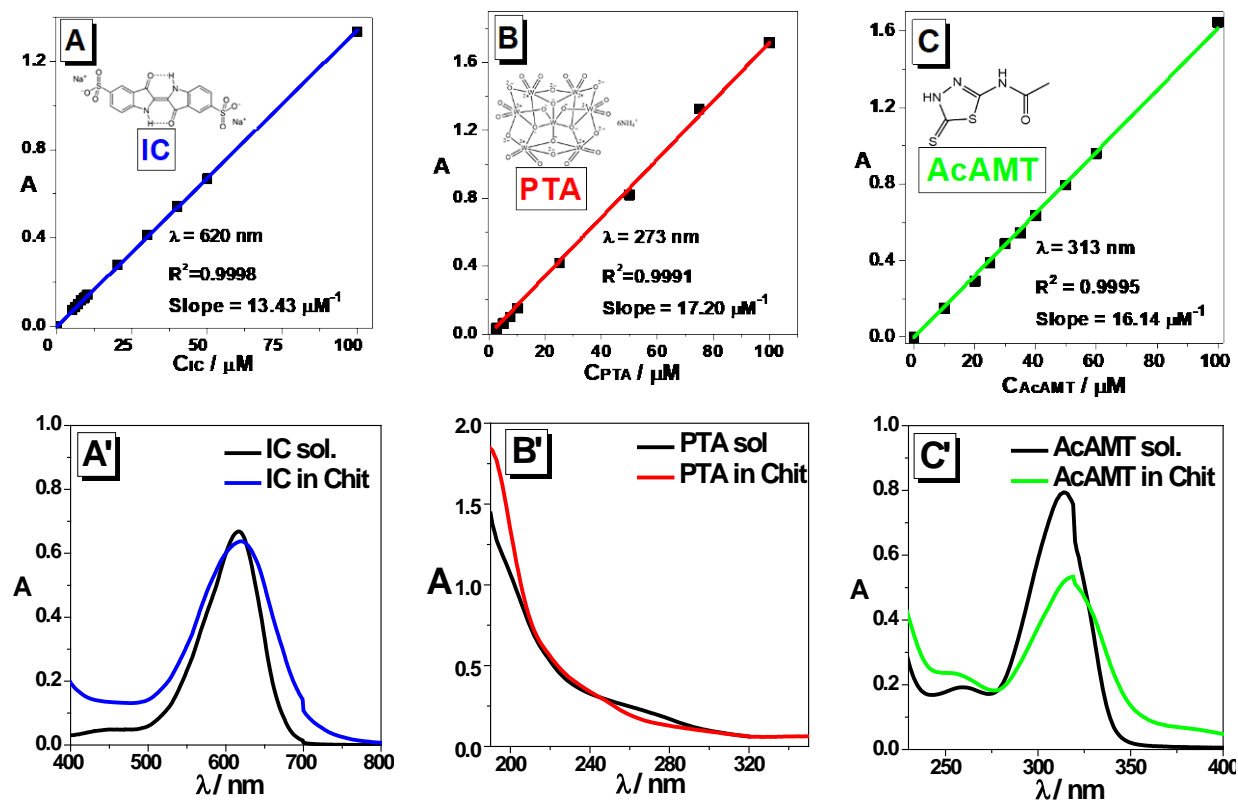
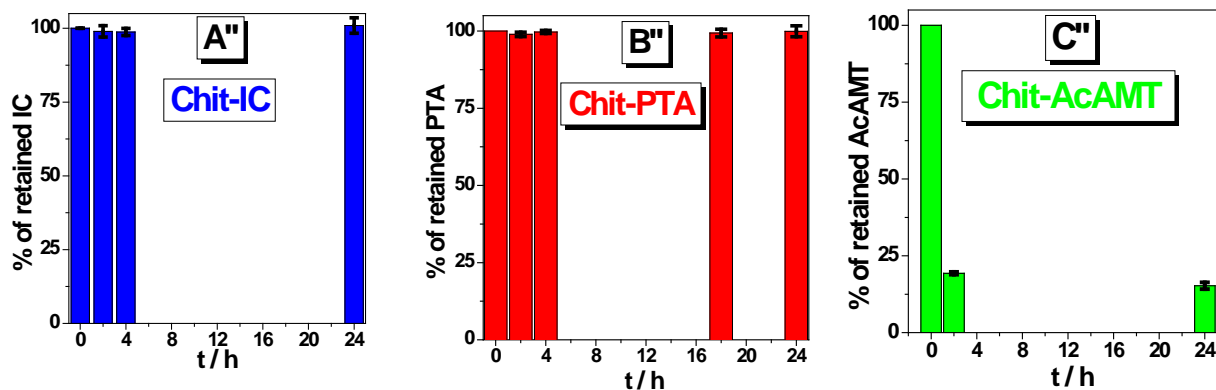*Figure 57: UV-Vis calibration curves (**A**) of impregnating agents (**blue-IC**; **red-PTA**; **green-AcAMT**) in aqueous solutions; absorbance spectra of impregnating agents in an aqueous solution vs. impregnated in a chitosan coating (**B**); stability of impregnated systems when exposed to distilled water (**C**).*

2.2.4.3. *Electrochemical investigation of the anticorrosive properties*

The anticorrosive properties of the impregnated chitosan coating were ascertained from the polarization curves and EIS measurements, compiled in Figure 64 and Table 6.

The presence of the impregnated chitosan coatings increased the polarization resistance in all studied cases (12880 Ωcm^2 for Zn/Chit-IC, 5537 Ωcm^2 for Zn/Chit-PTA and 6676 Ωcm^2 for Zn/Chit-AcAMT compared to 1957 Ωcm^2 for bare zinc). Additionally, it can be observed that the polarization resistance values determined by the linear polarization method and from the Nyquist spectra for both Zn/Chit-IC and Zn/Chit-AcAMT are in good accordance with each other.

Neither native chitosan, nor the 10^{-3} M inhibitor solutions resulted in improved characteristics, while coating zinc with the Chit-IC, Chit-PTA and Chit-AcAMT systems resulted in decreased corrosion current densities. Additionally, a strong drop in the current in the cathodic region of the polarization curves can be observed when ionic crosslinking agents were applied, as the reduced permeability of the coatings hinders oxygen diffusion.

The protective capabilities of the impregnated coatings can also be observed through the Nyquist impedance spectra, where the diameter of the capacitive loop is greatly increased for all impregnated systems.

The modest anticorrosive properties of the unmodified chitosan (28.63%) were greatly improved by reducing the permeability of the coatings through ionic crosslinking (97.52% for

Zn/Chit-IC and 97.91% for Zn/Chit-PTA [Szőke et al., 2019b]) or the accumulation of the AcAMT inhibitor in the vicinity of the metal surface (90.93%)
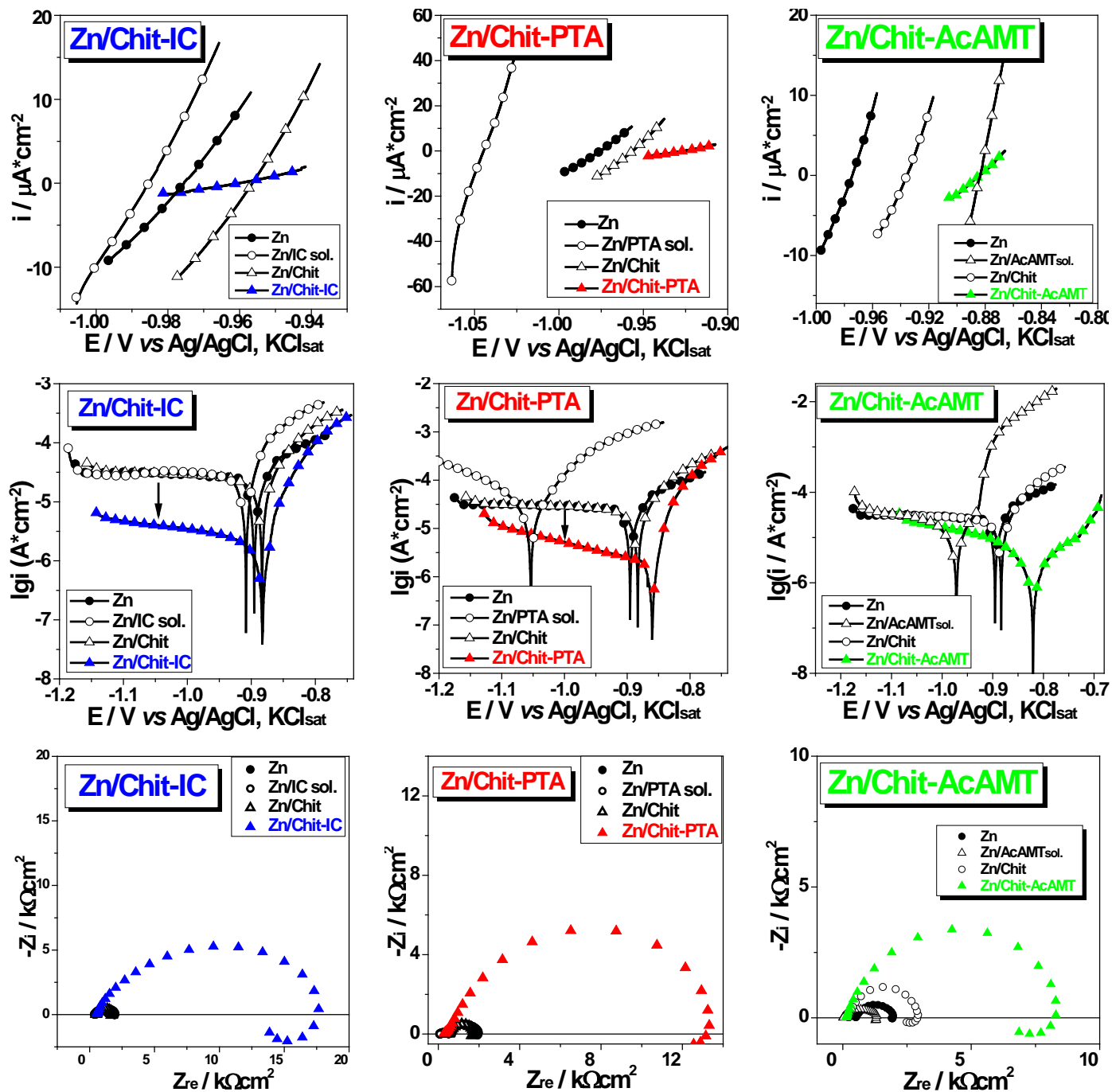

*Figure 64: Linear polarization curves, semilogarithmic polarization curves and Nyquist impedance spectra of bare Zn (●), bare Zn in the presence of 10^{-3} M of the impregnating agents (○), chitosan-coated Zn (Δ) and chitosan-coated Zn (▲) impregnated with **indigo carmine***

(blue), ammonium paratungstate (red) and AcAMT (green).

Experimental conditions: 0.2 g/L aqueous Na_2SO_4 solution, pH=5, scan rate, 0.166 mV/s, OCP, 60 minutes

*Table 6: Corrosion parameters of Zn, Zn in the presence of 10^{-3} M of the impregnating agents, chitosan-coated Zn and chitosan-coated Zn impregnated with **indigo carmine (blue)**, **ammonium paratungstate (red)** and **AcAMT (green)** determined from polarization curves*

Sample	E_{corr} from lin. pol.	E_{corr}	b_c	b_a	i_{corr}	Rp from lin. pol.	Rp from EIS	IE (%)
	V vs. RE	V vs. RE	V/dec	V/dec	μAcm^{-2}	Ωcm^2	Ωcm^2	
Zn	-0.965	-0.893	-	0.188	41.56	1957	1964	-
Zn/Chit	-0.956	-0.883	-	0.139	29.66	1558	2035	28.63
Zn/IC sol.	-0.985	-0.909	-	0.117	34.96	1395	1455	15.88
Zn/PTA sol.	-1.045	-1.053	-	0.194	215.72	512	391	-419.06
Zn/AcAMT sol.	-0.975	-0.971	0.303	0.038	11.08	1172	1325	73.33
Zn/Chit-IC	**-0.943**	**-0.883**	**0.647**	**0.042**	**1.03**	**12880**	**17660**	**97.52**
Zn/Chit-PTA	**-0.937**	**-0.860**	**0.349**	**0.030**	**0.87**	**5537**	**13368**	**97.91**
Zn/Chit-AcAMT	**-0.884**	**-0.817**	**0.151**	**0.137**	**3.77**	**6676**	**8290**	**90.93**

2.2.4.4.   Long term anticorrosive effect

Long term anticorrosive effects were investigated by EIS and microscopy measurements. Samples were exposed to a corrosive environment (0.2 g/L aqueous Na_2SO_4 solution).

After 3 days of exposure, microscopy images show a rough, uneven surface with crevices in the case of the Zn/Chit samples. For all impregnated samples, however, the structural integrity was retained, while the topography maps show even surfaces with no visible defects.
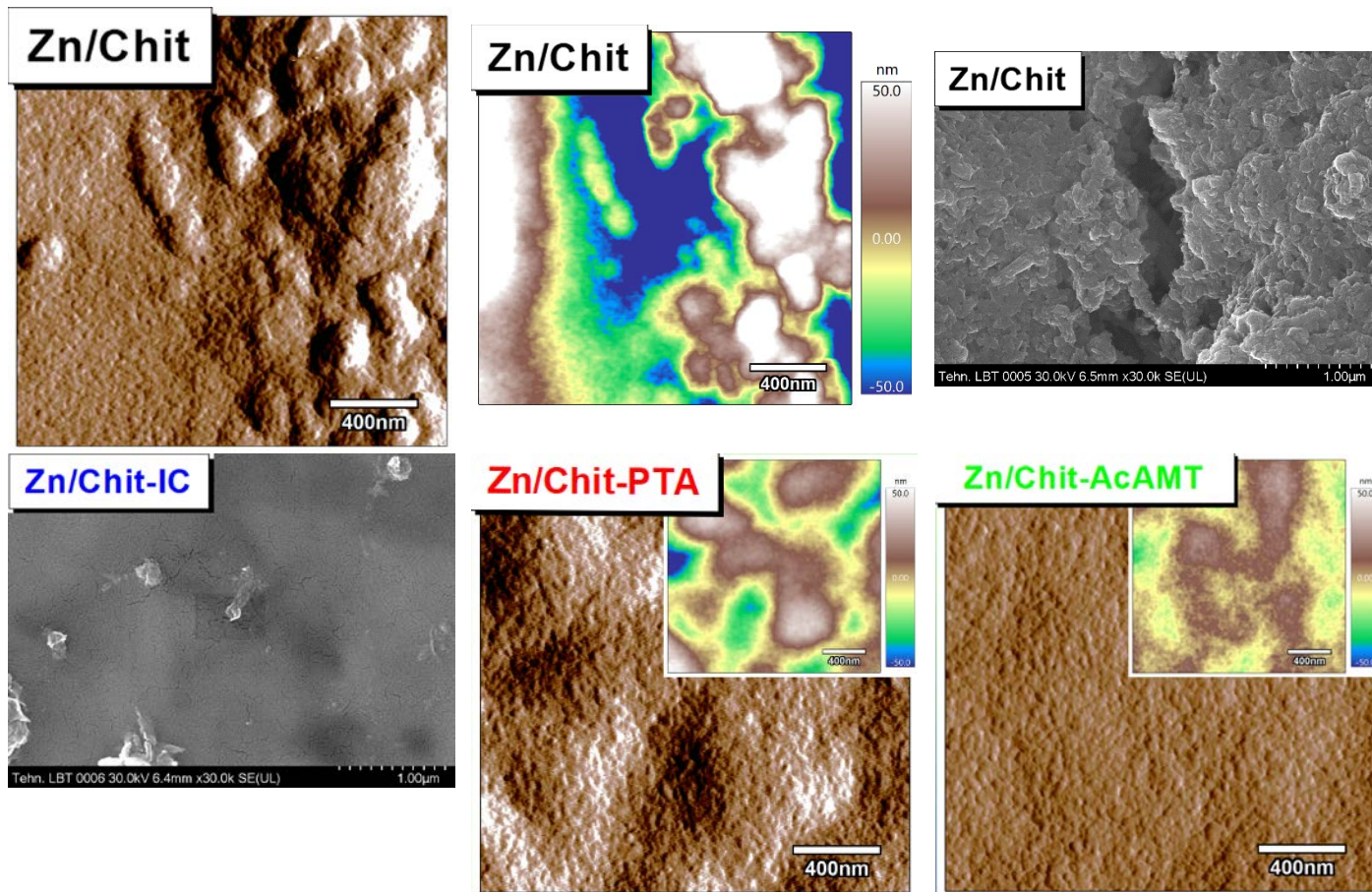
*Figure 68: SEM micrographs, AFM images and high-resolution topographies of **Zn/Chit**, **Zn/Chit-IC, Zn/Chit-PTA** and **Zn/Chit-AcAMT** samples after 3 days of exposure to 0.2 g/L Na$_2$SO$_4$ solution*

2.3.   Partial conclusions

By accumulating large amounts of corrosion inhibitors in the protective coating, highly efficient ionic crosslinking (in the case of PTA and IC) or surface adsorption (in the case of AcAMT) was achieved, improving the protective barrier against the corrosive environment.

The chitosan layers and the impregnation effectiveness were characterized by UV-Vis spectroscopy and EDS measurements, showing significant accumulation.

Electrochemical investigations assigned high inhibition efficiencies to all impregnated systems (>90%). EIS and polarization studies were corroborated with AFM and SEM studies which also show a retained structural integrity in the case of the modified coatings following exposure to a corrosive environment.

3. Anticorrosive silica-chitosan nanoparticle coatings produced with electrophoretic deposition

In an attempt to prepare new corrosion-resistant coatings, silica nanoparticles covered with chitosan were electrodeposited on a zinc cathode by electrophoresis from a 0.3 M NaCl solution to form a protective layer. The characteristics of the nanoparticles and of the resulting coatings are presented in what follows.

3.2.4.2. *Polarization studies*

Linear and semilogarithmic polarization curves (Figure 81) show an increase in polarization resistance and decrease in current densities for the coated samples. Inhibition efficiencies calculated from the polarization curves of the systems demonstrate that a 30-minute deposition only offers a relatively modest protection with an IE of 63.91%. This is improved by 90 minutes of ED significantly to, 76.90% (Table 13). Nevertheless, results fall short of the anticorrosive effects exhibited by chitosan layers produced by dip-coating (see Section 2.2.).
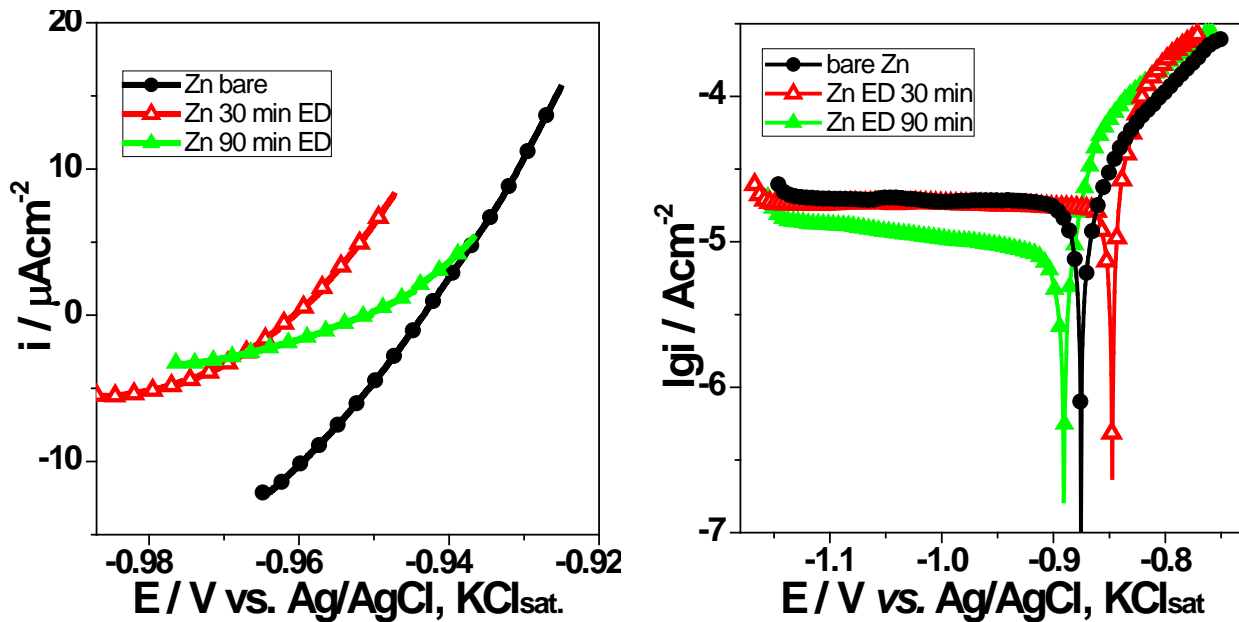

Figure 81: Linear (A) and semilogarithmic (B) polarization curves (current density vs. potential) of bare Zn (black ●), Zn – ED 30min (red △) and Zn – ED 90min (green ▲) systems Experimental conditions: 0.2 g/L Na2SO4 solution, scan rate, 0.166 mV/s, OCP, 60 minutes.

Table 13: Corrosion parameters for various coated Zn samples determined by polarization

Sample	E_{corr} from lin. pol.	E_{corr}	b_c	b_a	i_{corr}	Rp from lin. pol.	Rp from EIS	IE (%)
	V vs. RE	V *vs*. RE	V/dec	V/dec	μAcm^{-2}	Ωcm^2	Ωcm^2	
bare Zn	-0.965	-0.893	-	0.188	41.56	1957	1964	-
Zn - ED 30 min	-0.961	-0.847	-	0.133	15.00	2242	3853	63.91
Zn - ED 90 min	-0.951	-0.891	0.949	0.165	9.60	4537	6356	76.90

3.3. Partial conclusions

The electrochemical investigations highlighted improved corrosion resistances for both coated systems, with the higher anticorrosive protection manifesting at samples coated with 90 minutes of ED. The inhibition efficiencies calculated, however, are still relatively low, compared to chitosan coatings produced with other methods (Section 2.1.2.), demonstrating that thin layers formed by ED of lmwChit-silica nanoparticles do not constitute a viable alternative in the anticorrosive protection of zinc substrates.

4. General conclusions

I. Two new **modified glassy carbon electrodes**, based on graphenes were produced with the drop casting method. Following optimization studies, the resulting GCE/Chit/Chit-rGO-Mb and GCE/AuNPs-erGO-Nafion interfaces were used to determine H_2O_2 and L-ascorbic acid, respectively.

- The modified GCE/Chit/Chit-rGO-Mb was successfully applied for H_2O_2 detection. Immobilizing rGO at the electrode surface slightly reduced the detection limit for H_2O_2 from 7.75 μM to 7.09 μM, and increased the sensitivity.

- In the case of the GCE/AuNPs-erGO-Nafion modified electrode, good electrocatalytic activity (due to the synergistic effect of erGO and gold nanoparticles) and selectivity were observed in AA determination. The

GCE/AuNPs-erGO-Nafion electrode was used successfully in the electrochemical analysis of AA from pharmaceutical products.

II. Native chitosan coatings have limited applicability in anticorrosive protection due to the high permeability of the polymer. Thus, in an attempt to improve the anticorrosive properties of chitosan layers, three different modifying agents were accumulated in **chitosan coatings** produced with the dip-coating method on zinc substrates (IC, PTA and AcAMT). The resulting impregnated systems show good anticorrosive characteristics based on either ionic crosslinking (for IC and PTA) or the promotion of inhibitor adsorption on the metal surface (in the case of AcAMT).

The studies highlight the applicability of EIS measurements in the characterization of thin polymer coatings.

Chit-IC, Chit-PTA and Chit-AcAMT coatings all show good inhibition efficiencies (>90%) and could be applied successfully in the temporary protection of zinc parts during transport.

III. **Chitosan-silica nanoparticle coatings** were deposited on zinc plates using electrophoretic deposition. Even after optimization, results showed an uneven deposition of nanoparticles. Electrochemical investigations highlighted some anticorrosive effect from the nanoparticle coatings that is improved by an increased amount of ED time, however, results still fall short of inhibition efficiencies obtained with other methods.

Scientific activity
Papers published

1.	**Szőke**, **Á.F.;** Szabó, G.S.; Hórvölgyi, Z.; Albert, E.; Gaina, L.; Muresan, L.M., Carbohydrate Polymers, 215 (**2019**), 63-72.

2.	**Szőke**, **Á.F.;** Szabó, G.; Hórvölgyi, Z.; Albert, E.; Végh, A.G.; Zimányi, L.; Muresan, L.M., International Journal of Biological Macromolecules (**accepted**)

3.	**Szőke**, **Á.F.;** Szabó, G.; Simó, Z.; Hórvölgyi, Z.; Albert, E.; Végh, A.G.; Zimányi, L.; Muresan, L.M., European Polymer Journal, 118 (**2019**), 205-212.

4. **Szoke**, **A.;** Zsebe, Z.; Turdean, G.L.; Muresan, L.M., Electrocatalysis, 10(5) (**2019**), 573-583.

5. **Szőke, Á.;** Turdean, G.; Muresan, L., Bulgarian Chemical Communications, 49 (**2017**), 147-154.

6. **Szőke, Á.F.;** Mureşan, L.M.; Turdean, G.L.; Zsebe, Z.; Ablaeva, K., in Proceedings of the 23rd International Symposium on Analytical and Environmental Problems", pp. 334-337 (**2017**),

7. **Szőke, Á.F.;** Kerekes, E.; Timár, D.K.; Turdean, G.L.; Mureşan, L.M.; Szabó, G.; Barabás R., Acta Scientiarum Transylvanica, 25(3) (**2017**), 72-79.

8. Várhelyi Jr., Cs.; Lengyel, A.; Homonnay, Z.; Szalay, R.; Pokol, Gy.; Szilágyi, I.-M.; Huszthy, P.; Papp, J.; Giga, F.; Golban, L.-M.; Várhelyi, M.; Tomoaia-Cotisel, M.; **Szőke, Á.;** Kuzmann, E., Hyperfine interactions, 238:87 (**2017**).

9. Szabó, G.; Albert, E.; Both, J.; Kócs, L.; Sáfrán, Gy.; **Szöke**, **A.;** Hórvölgyi, Z.; Mureşan L.M., Surfaces and Interfaces, 15 (2019), 216-223.

10. **Szőke**, **Á.F.;** Szabó, G.; Hórvölgyi, Z.; Albert, E., Acta Scientiarum Transylvanica, 26(3) (**2019**), 38-46.

11. **Szőke**, **Á.F.;** Szabó, G.; Hórvölgyi, Z.; Albert, E., Acta Scientiarum Transylvanica (**submitted**)

Conference participations

- **Oral presentations**

1. **Szőke**, **Á.F.;** Sanders, Q.J.; Szabó, G.S.; Muresan, L.M.; Turdean, G.L., 22nd International Conference on Chemistry, November **2016**, Timisoara, Romania

2. **Szőke**, **Á.F.,** Kerekes, E., Timár, D.K., Turdean, G.L., Muresan, L.M., Szabó, G.S.; Barabás R., 15th Transylvanian Conference of Natural Science, November **2016**, Cluj-Napoca, Romania

3. **Szőke**, **Á.F.** **;** Turdean, G.L., 33rd National Student Conference (OTDK), March **2017**, Miskolc, Hungary

4. **Szőke**, **Á.F.;** Szabó, G.S.; Albert, E.; Hórvölgyi, Z.; Muresan, L.M., 6th RSE-SEE international conference, June **2017**, Balatonkenese, Hungary

5. **Szőke**, **Á.F.;** Szabó, G.S.; Muresan, L.M.; Albert, E.; Hórvölgyi, Z., 22nd International Conference on Chemistry, October **2017**, Deva, Romania

6. **Szőke**, **Á.F.;** Szabó, G.S.; Muresan, L.M.; Hórvölgyi, Z.; Albert, E., 16th Transylvanian Conference of Natural Science, November **2017**, Cluj-Napoca, Romania

7. **Szőke**, **Á.F.;** Szabó, G.S.; Albert, E.; Muresan, L.M.; Hórvölgyi, Z., 11th Conference on Colloid Chemistry – 11CCC, Mai **2018**, Eger, Hungary

8. **Szőke**, **Á.F.;** Zsebe, Z.; Turdean, G.L.; Muresan, L.M., 69th Annual Conference of the International Society of Electrochemistry, September **2018**, Bologna, Italy

9. **Szőke**, **Á.F.;** Szabó, G.S.; Muresan, L.M.; Albert, E.; Hórvölgyi, Z., 24th International Conference on Chemistry, October **2018**, Sovata, Romania

10. **Szőke**, **Á.F.;** Szabó, G.S.; Muresan, L.M.; Hórvölgyi, Z.; Albert, E., 17th Transylvanian Conference of Natural Science, November **2018**, Cluj-Napoca, Romania

11. **Szőke**, **Á.F.;** Bliet, G.; Szabó, G.; Muresan, L., Interdiszciplinaritás a Kárpát-Medencében, PhD conference, Mai **2019**, Pécs, Hungary

12. **Szőke**, **Á.F.;** Szabó, G.S.; Hórvölgyi, Z.; Albert, E.; Muresan, L.M., Mai **2019**, Split, Croatia

- **Poster presentations**

13. **Szőke, Á.F.;** Muresan, L.M.; Turdean, G.L.; Zsebe, Z.; Ablaeva, K., 23rd International Symposium on Analytical and Environmental Problems, October **2017**, Szeged, Hungary

14. Zsebe, Z.; **Szőke, Á.F.;** Muresan, L.M.; Turdean, G.L., 23rd International Conference on Chemistry, October **2017**, Deva, Romania

15. Simó, Z.; **Szőke**, **Á.;** Albert, E.; Hórvölgyi, Z.; Szabó, G.; Muresan, L., 15th Students for students international conference, April **2018**, Cluj-Napoca, Romania

16. Both, J.; **Szőke**, **Á.;** Albert, E.; Hórvölgyi, Z.; Muresan, L., Gabriella Szabó, 15th Students for students international conference, April **2018**, Cluj-Napoca, Romania

Selected references

1. Albert, E.; Cotolan, N.; Nagy, N.; Sáfrán, Gy.; Szabó, G.; Mureşan, L.M.; Hórvölgyi, Z., Microporous and Mesoporous Materials, 206 (**2015**), 102-113.

2. Amidon, G.E.; Meyer, P.J.; Mudie, D.M., Developing Solid Oral Dosage Forms, Academic Press (**2017**), 271-293.

3. Antuña-Jiménez, D.; Díaz-Díaz, G.; Blanco-López, M.C.; Lobo-Castañón, M.J.; Miranda-Ordieres, A.J.; Tuñón-Blanco, P., Molecularly Imprinted Sensors, Elsevier (**2012**), 1-34.

4. Asahi, T.; Uwada, T.; Masuhara, H., Handai Nanophotonics, 2, Elsevier (**2006**), 219-228.

5. Bastidas, D.M.; Criado, M.; Bastidas, J.-M., Nanocoatings and Ultra-Thin Films, Woodhead Publishing (**2011**), 131-156.

6. Belfar, M.L.; Lanez, T.; Rebiai, A.; Ghiaba, Z., International Journal of Electrochemical Science, 10 (**2015**), 9641 – 9651.

7. Berger, J.; Reist, M.; Mayer, J.M.; Felt, O.; Peppas, N.A.; Gurny, R., European Journal of Pharmaceutics and Biopharmaceutics, 57 (**2004**), 19–34.

8. Berne, B.J.; Pecora, R., Courier Dover Publications, Mineola (**2000**).

9. Bhambhani, A.; Thakkar, S.; Joshi, S.B.; Middaugh, C.R., Therapeutic Protein Drug Products, Woodhead Publishing (**2012**), 13-45.

10. Bovin, N.V.; Gabius, H.J., Chemical Society Reviews, 24 (**1995**), 413-421.

11. Chandran, P.R.; Thomas, R.T., Nanotechnology Applications for Tissue Engineering, William Andrew Publishing (**2015**), 221-237.

12. Chelaru, J.; Muresan, L., Studia Universitatis Babes-Bolyai Chemia, 59 (**2014**), 91-102.

13. Ching, Y.C.; Gunathilake, T.M.S.U.; Ching, K.Y.; Chuah, C.H.; Sandu, V.; Singh, R.; Liou, N.S., Durability and Life Prediction in Biocomposites, Fibre-Reinforced Composites and Hybrid Composites, Woodhead Publishing (**2019**) 407-426.

14. Chooto, P., IntechOpen (**2019**)

15. Dabóczi, M.; Albert, E.; Agócs, E.; Kabai-Faix, M.; Hórvölgyi, Z., Carbohydrate Polymers, 136 (**2016**), 137-145.

16. Deture, F.A.; Drylie, D.M., The Journal of Urology, 112(6) (**1974**), 693-696.

17. dos Anjos, F.S.C.; Vieira, E.F.S.; Cestari, A.R., Journal of Colloid and Interface Science, 253 (**2002**), 243–246.

18. Ebnesajjad, S., Surface Treatment of Materials for Adhesive Bonding, 2nd Edition, William Andrew Publishing (**2014**), 39-75.

19. Eng, A.Y.S.; Chua, C.K.; Pumera, M., Electrochemistry Communications, 59 (**2015**), 86-90.

20. Feng, L.; Iroh, J.O., Journal of Applied Polymer Science, 135 (**2018**), 45861.

21. Food Standards Agency, Current EU approved additives and E Numbers, **2019**

22. Griffete, N.; Frederich, H.; Maître, A.; Ravaine, S.; Chehimi, M.M.; Mangeney, C., Langmuir, 28 (**2012**), 1005-1012.

23. Hanifah, I.; Yuliasari, F.; Fitrilawati, F.; Syakir, N.; Hidayat, S.; Safriani, L.; Bahtiar, A.; Aprilia, A.; Siregar, R.E., Journal of Physics Conference Series, 1080(1) (**2018**), 012025.

24. Hanson, K.M.; Pappas, T.J.; Holland, L.A., Comprehensive Analytical Chemistry, 45, Elsevier (**2005**), 413-440.

25. Harvey, J.W., Clinical Biochemistry of Domestic Animals, Academic Press (**2008**), 259-285.

26. Heinze, J., Angewandte Chemie, 23 (**1984**), 831-847.

27. Hild, E.; Deák, A.; Naszályi, L.; Sepsi, Ö.; Ábrahám, N.; Hórvölgyi, Z., Journal of Optics A: Pure and Applied Optics, 9 (**2007**), 920-930.

28. Honeychurch, K.C., Printed Films, Woodhead Publishing (**2012**), 366-409.

29. Instant Cheminformatics Solutions, **2019**

30. Kekedy, L.; Kekedy, N.L., Műszeres analitikai kémia I-III, Erdélyi Múzeum Egyesület, Kolozsvár (**1995**)

31. Kerdi, F.; Caps, V.; Tuel, A., Studies in surface science and catalysis, 175, Elsevier (**2010**), 221-224.

32. Koch, G.; Varney, J.; Thompson, N.; Moghissi, O.; Gould, M.; Payer, J., Nace International, International Measures of prevention, application, and economics of corrosion technologies study, **2016**

33. Krstic, M.; Medarevic, D.; Duris, J.; Ibric, S., Lipid Nanocarriers for Drug Targeting, William Andrew Publishing (**2018**), 473-508.

34. Le Pevelen, D.D., Encyclopedia of Spectroscopy and Spectrometry, Academic Press, (**2017**), 98-109.

35. Lin, V.S.; Dickinson, B.C.; Chang, C.J., Methods in Enzymology, 526, Academic Press (**2013**), 19-43.

36. Lotfi, M.; Nejib, M.; Naceur, M., Intech (**2013**), 207-240.

37. Lyons, M.E.G., Electroanalysis, 27(4) (**2015**), 992-1009.

38. Mirkhalaf, F.; Graves, J.E., Chemical Papers, 66 (**2012**), 472-483.

39. Mohr, G.J., Optical Chemical Sensors, Springer, Dordrecht (**2006**).

40. Palm Sens, Tafel Plot and Evans Diagram, **2019**

41. Pang, X.; Zhitomirsky I., Surface and Coatings Technology, 202 (16) (**2008**), 3815-3821.

42. Polini, A.; Yang, F., Nanofiber Composites for Biomedical Applications, Woodhead Publishing (**2017**), 97-115.

43. Quintino, L., Surface modification by solid state processing, Woodhead Publishing (**2014**), 1-24.

44. Raicopol, M.; Branzoi, V.; Necula, L.; Ionita, M.; Pilan, L., Revue Roumaine de Chimie, 57(9-10) (**2012**), 807-814.

45. Schwarz, A.; Van Langenhove, L., Multidisciplinary know-how for smart-textiles developers, Woodhead Publishing (**2013**), 29-69.

46. Shao, M.; Chang, Q.; Dodelet, J.P.; Chenitz, R., Chemical reviews, 116(6) (**2016**), 3594-3657.

47. Shetti, N.P.; Nayak, D.S.; Reddy, K.R.; Aminabhvi, T.M., Graphene-Based Electrochemical Sensors for Biomolecules, Elsevier (**2019),** 235-274.

48. Shi, L.; Liang, R.-P.; Qiu, J.-D., Journal of Materials Chemistry, 22 (**2012**), 17196-17203.

49. Siqueira, J.R.; Oliveira, O.N., Nanostructures, William Andrew Publishing (**2017**), 233-249.

50. Song, J.; Xu, L.; Xing, R.; Li, Q.; Zhou, C.; Liu, D.; Song, H., Scientific Reports, 4 (**2014**), 7515.

51. **Szőke**, **Á.;** Turdean, G.; Muresan, L., Bulgarian Chemical Communication, 49 (**2017**), 147-154.

52. **Szőke**, **Á. F.;** Szabó, G. S.; Hórvölgyi, Z.; Albert, E.; Gaina, L.; Muresan, L. M., Carbohydrate Polymers, 215 (**2019a**), 63-72.

53. **Szoke**, **A.;** Zsebe, Z.; Turdean, G.L.; Muresan, L. M., Electrocatalysis, 10(5) (**2019c**), 573-583.

54. **Szőke**, **Á.F.;** Szabó, G.; Simó, Z.; Hórvölgyi, Z.; Albert, E.; Végh, A. G.; Zimányi, L.; Muresan, L. M., European Polymer Journal, 118 (**2019b**), 205-212.

55. **Szőke**, **Á.F.;** Turdean, G.L.; Katona, G.; Muresan, L.M., Studia Universitatis Babes-Bolyai Chemia, 61(3), Tom I (**2016**), 135-144.

56. Thissen, H., Biosynthetic Polymers for Medical Applications, Woodhead Publishing (**2016**), 129-144.

57. Varvara, S.; Muresan, L.M.; Rahmouni, K.; Takenouti, H., Corrosion Science, 50(9) (**2008**), 2596-2604.

58. Ziyatdinova, G.; Ziganshina, E.; Budnikov, H., Talanta, 99 (**2012**), 1024-1029.